NASA CR-147565
ERIM 109600-45-F

Final Report

RADAR DATA PROCESSING AND ANALYSIS

D. AUSHERMAN, R. LARSON, and C. LISKOW
Radar and Optics Division

FEBRUARY 1976

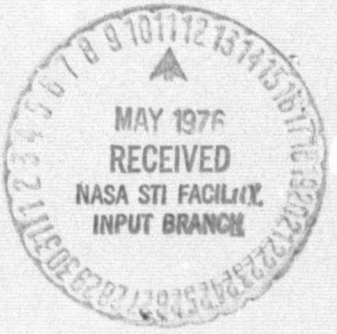

Prepared for

NATIONAL AERONAUTICS AND SPACE ADMINISTRATION

Lyndon B. Johnson Space Center
Houston, Texas 77058
Contract No. NAS9-14123, Task I

ENVIRONMENTAL
RESEARCH INSTITUTE OF MICHIGAN
FORMERLY WILLOW RUN LABORATORIES, THE UNIVERSITY OF MICHIGAN
BOX 618 • ANN ARBOR • MICHIGAN 48107

TECHNICAL REPORT STANDARD TITLE PAGE

1. Report No.	2. Government Accession No.	3. Recipient's Catalog No.
109600-45-F		

4. Title and Subtitle	5. Report Date
RADAR DATA PROCESSING AND ANALYSIS	February 1976
	6. Performing Organization Code

7. Author(s)	8. Performing Organization Report No.
D. Ausherman, R. Larson, and C. Liskow	109600-45-F

9. Performing Organization Name and Address	10. Work Unit No.
Radar and Optics Division Environmental Research Institute of Michigan P.O. Box 618 Ann Arbor, Michigan 48107	Task I
	11. Contract or Grant No. NAS9-14123
	13. Type of Report and Period Covered Final Report 15 May 1974 - 14 March 1975
12. Sponsoring Agency Name and Address Lyndon B. Johnson Space Center National Aeronautics and Space Administration Houston, Texas 77058	14. Sponsoring Agency Code

15. Supplementary Notes

16. Abstract

On April 5, 1974, the Environmental Research Institute of Michigan's (ERIM) dual-polarized X- and L-band Synthetic Aperture Radar was flown to collect radar imagery of the Phoenix, Arizona soil-moisture test site. In September, 1973, an earlier mission was flown over the Huntington, Indiana agricultural test site. The primary objective of the work reported here was to generate digitized four-channel radar images corresponding to particular areas from the Phoenix and Huntington test sites. The methods for generating this imagery are documented. The primary objective has been completed and the resulting data supplied to NASA/JSC and to the University of Kansas Remote Sensing Laboratory.

A secondary objective to be pursued, following the delivery of the digitized radar data, was the investigation of digital processing techniques for extraction of information from the multibond radar image data. Following the digitization, the remaining resources permitted a preliminary machine analysis to be performed on portions of the radar image data. The results, although necessarily limited, are reported here.

17. Key Words	18. Distribution Statement
Synthetic Aperture Radar (SAR) Digital image processing Multi-channel SAR Radar data analysis Remote sensing Soil-moisture measurement	Initial distribution is indicated at the end of this document.

19. Security Classif. (of this report)	20. Security Classif. (of this page)	21. No. of Pages	22. Price
UNCLASSIFIED	UNCLASSIFIED	58	

PREFACE

This document is a final technical report of work supported by the National Aeronautics and Space Administration's Lyndon B. Johnson Space Center under Contract No. NAS9-14123, Task I. The Principal Investigator for Task I was D. A. Ausherman.

The report was prepared by members of the Radar and Optics Division of the Environmental Research Institute of Michigan, P.O. Box 618, Ann Arbor, Michigan 48107. The optical radar data processing and digitization described in this work was performed by A. Klooster. The development and application of the digital-computer image registration and tape-formatting capabilities was the responsibility of L. Wilock. In addition, L. Wilock, C. Davis, and L. Bryan made significant contributions to the analysis of the multi-channel radar data.

CONTENTS

FIGURES

TABLES

RADAR DATA PROCESSING AND ANALYSIS

1
INTRODUCTION

The primary objective of the Radar Data Processing and Analysis Task was to generate four-channel digital radar imagery corresponding to particular scenes from the Phoenix, Arizona soil moisture test site and the Huntington, Indiana agricultural test site. A secondary objective, to be pursued following the completion of the radar data digitization on a resources-available basis, was the investigation of digital processing techniques for extraction of information from the multiband radar image data. The primary objective was successfully completed with the shipment of radar-image data tapes to NASA/JSC and the University of Kansas Remote Sensing Laboratory. In addition, the remaining resources permitted a preliminary machine analysis to be performed on portions of the radar-image data.

The four-channel radar data consists of imagery made at two wavelengths, 3.2 cm (X-band) and 23.0 cm (L-band), with two polarization configurations for each wavelength. For each wavelength, horizontally polarized pulses are transmitted and both horizontally and vertically polarized returns are recorded on signal film. Thus, the four channels are (1) X-band horizontal-horizontal, (2) X-band horizontal-vertical, (3) L-band horizontal-horizontal, and (4) L-band horizontal-vertical. For brevity the notations X(HH), X(HV), L(HH), and L(HV) will be used to designate the four radar channels.

The radar signal data is recorded on signal films aboard the aircraft in the form of dispersed two-dimensional signals which must be further processed to form an image. Currently, the required two-dimensional signal processing is performed using a coherent optical data processor. In the present case, the output of the optical processor was digitized directly using an image dissector camera, and the resultant image data were written on computer-compatible tapes. Direct digitization provides a greater dynamic range in output than would be possible if the image were recorded on film and subsequently digitized. After digitization, the four channels of imagery must be spatially registered prior to interlacing and recording on a single magnetic tape. This report will document the procedures used for registering and formatting the four-channel radar-image data.

Following the completion of the image digitization and registration task, selected portions of the multiband radar-image data were subjected to machine analysis. Univariate statistics from single channels were extracted from individual fields and analyzed with respect to field content. In addition, linear discriminate analysis was applied to the fields to determine the separability of dry versus wet areas. Adjacent-cell averaging procedures were applied to improve the performance of the discrimination techniques. The results of the preliminary data analysis are presented in Section 3.3

2
IMAGE PROCESSING, DIGITIZATION, AND REGISTRATION

In order to produce digital imagery, each signal history is processed on a coherent optical processor, the output of which is digitized using an electronically scanned image dissector camera. Since current optical processors are inherently single-channel devices, each channel of the multiband radar signals must be processed and digitized individually. This process introduces between-channel spatial misregistration (primarily translational) which must be removed to produce meaningful multiband image data. This section will review the procedures used to process, digitize, and register the image data. A summary of the digital image data provided to both NASA/JSC and Kansas will be given.

2.1 RADAR DATA PROCESSING AND DIGITIZATION

The concept of Synthetic Aperture Radar (SAR) is well documented [1-3]. The SAR utilized for the present experiment was the sidelooking radar configuration shown in Figure 1. The objective of such a system is to generate a two-dimensional continuous image of the terrain strip illuminated by a microwave beam as the radar vehicle moves in the azimuth (along-track) direction at a constant velocity. Range (cross-track) resolution is obtained by transmitting dispersed pulses and applying pulse compression techniques to the returned signals. Azimuth resolution is obtained by recording the Doppler frequency shifts associated with the returns from point scatterers as they migrate through the antenna beam. Knowledge of the Doppler

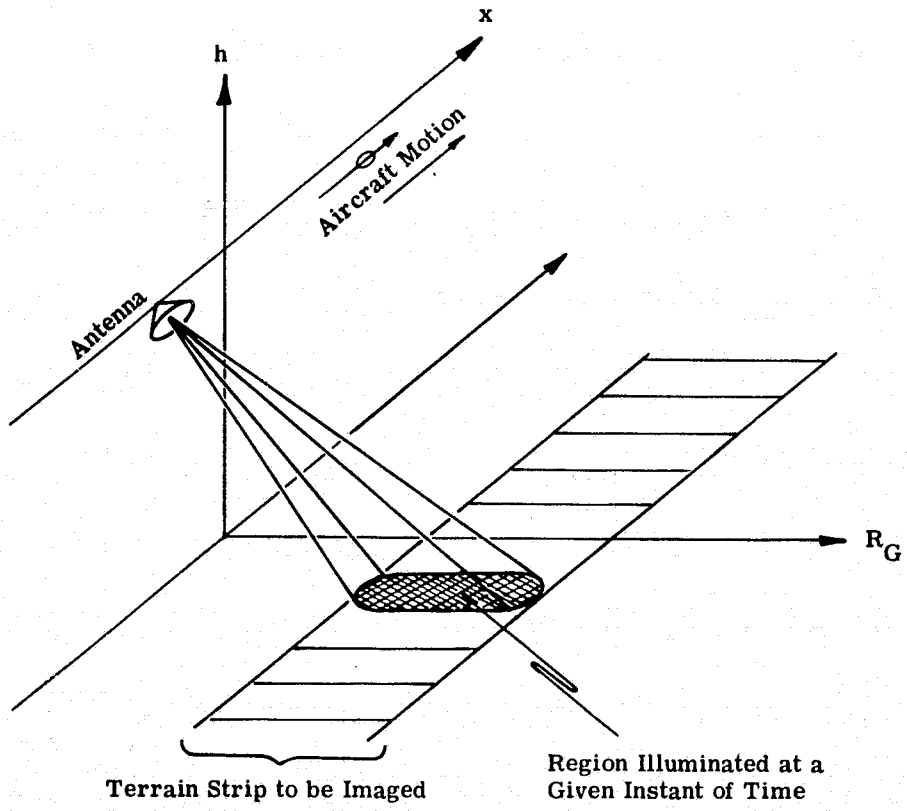

FIGURE 1. SCHEMATIC REPRESENTATION OF STRIP-MAP MODE IMAGING RADAR

frequency versus time relationship for a point scatterer at a given range allows one to precisely locate the scatterer in azimuth in a manner analogous to the pulse compression applied in the range direction. The uncompressed radar echoes are recorded and subsequent two-dimensional signal processing is applied to form an image.

For coherent optical signal compression, film is the usual storage medium. The radar returns are coherently mixed to video frequencies and used to modulate the intensity of a CRT spot as its image is swept across a photographic film at a constant velocity. The video signal maintains a small carrier frequency to avoid any spectral folding, and it is recorded about a D.C. bias level to enable the proper recording of bipolar signals. The resultant film recording is a linear correspondence between slant range (time-delay) and the spatial dimension across the film. Subsequent pulses are recorded side-by-side along the film as the film is moved past the CRT at a rate proportional to the radar vehicle velocity, as measured by the aircraft's inertial navigation system (INS). The spatial dimension along the signal film is therefore linearly related to the azimuth dimension of the terrain. The developed film forms the input to the optical processor. In the present case, the X-band signals are recorded on one film strip and the L-band signals on another.

The optical processor acts as a two-dimenional filter matched to the signal generated by a point scatterer. Thus, the required two-dimensional pulse compression can be viewed as the convolution of an appropriate reference function with the recorded radar signal. In the optical processor, this convolution is performed by configuring the lenses such that

the impulse response of the processor is identical to the desired reference function. The primary advantage of the optical approach is the nearly instantaneous processing capability for two-dimensional signals with very high information content.

The optical processing facility usually utilizes a configuration known as the tilted-plane optical processor. This optical system has been previously reported [4] and will not be described in detail here. For a brief description, consider the schematic diagram of the processor shown in Figure 2. A spherical telescope, usually of unity magnification, is comprised of spherical lenses L_1 and L_2. A cylindrical telescope of variable magnification, consisting of lenses L_3 and L_4 is in tandem. The signal-film transparency S is illuminated with collimated, monochromatic (laser) light by utilization of a point source P and collimator L_0. The desired image forms at the output plane I, where it is digitized by the use of an image dissector system. Frequency plane filtering can easily be accomplished by placing the appropriate slits and weighting masks in plane F, which is the spatial two-dimensional Fourier transform of the input data. Such filtering is used primarily to limit the passband of the processor. For certain forms of coded radar pulses, the desired matched filtering occurs as a consequence of the lens action and free space transformations associated with the optical configuration.

If the ranging signal transmitted by the radar is a linear frequency modulated (chirp) pulse, the slant-range image is formed near the signal film due to the propagation effects between the film and the image. This image is then reimaged via the spherical telescope to the output

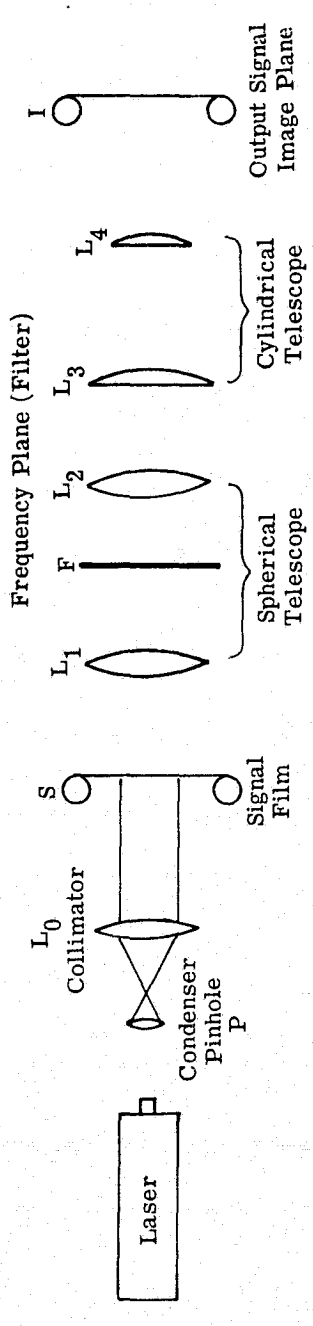

FIGURE 2. TILTED-PLANE PROCESSOR

plane I. The azimuth signal history is a true microwave hologram [3] which forms an image, usually in a different plane and of different magnification than the range image. By adjusting the magnification and the position of the cylindrical telescope (with no effect on the range image), the range and azimuth image planes can be brought into coincidence with unity aspect at plane I.

The above processing method is complicated in that the azimuth image plane is tilted with respect to the signal film, while the range image is parallel to the signal film.* The solution is to tilt the input and output planes the proper amount to bring the planes to a common focus [4]. When the input plane is rotated about the azimuth coordinate, the slant-range image formed by the unity telescope rotates the same amount. The azimuth image, however, is demagnified by the cylindrical telescope and therefore rotates a proportionally lesser amount. A tilt angle usually exists which brings the two image planes into focus.

Frequency plane filtering is required in the processor to remove the conjugate (the negative frequency band) and undiffracted (D.C.) wavefronts which result from the holographic signal recording. A frequency plane slit is used to ensure that these signal components do not corrupt the final image. In addition, aperture weighting masks can be inserted in the frequency plane to provide the desired processor impulse response. In the present experiment, an

*The azimuth image plane is tilted due to the fact that the Doppler frequency vs azimuth position relationship is a function of the range of the scatterer. This in turn implies that the azimuth holographic signals have focal lengths which vary linearly with range.

aperture was used to produce radar imagery with 9-m resolution in both range and azimuth.

Because the optical processor is inherently a single-channel device, each channel of the radar data is processed individually. The L-band and X-band films are each run through the processor twice to obtain the parallel and cross-polarized images. A different portion of the film is illuminated each time. This single-channel processing introduces spatial registration errors which must later be removed.

The radar processor used in this experiment was a hybrid facility in that the processor output is digitized directly rather than being recorded on film. This allows one to obtain greater dynamic range than would be possible by recording on film.

A block diagram of the hybrid facility is shown in Figure 3. The key to the optical-digital interface is the image dissector camera manufactured by ITT Aerospace/ Optical Division. The image dissector has been described as a photomultiplier with a small electronically movable photocathode area, thus acting as an all-electronic, low-inertia microphotometer. The dissector camera is positioned such that the output image of the optical processor is focused upon the photocathode. Electrons are emitted from the back of the photocathode, forming an electronic image with current density modulated according to the image input. The electron image, focused by magnetic deflection, falls upon an aperture plane at the other end of the drift tube. The aperture samples the image by allowing only a small, well-defined area of the electron image to pass through to the electron multiplier, which then multiplies the sampled

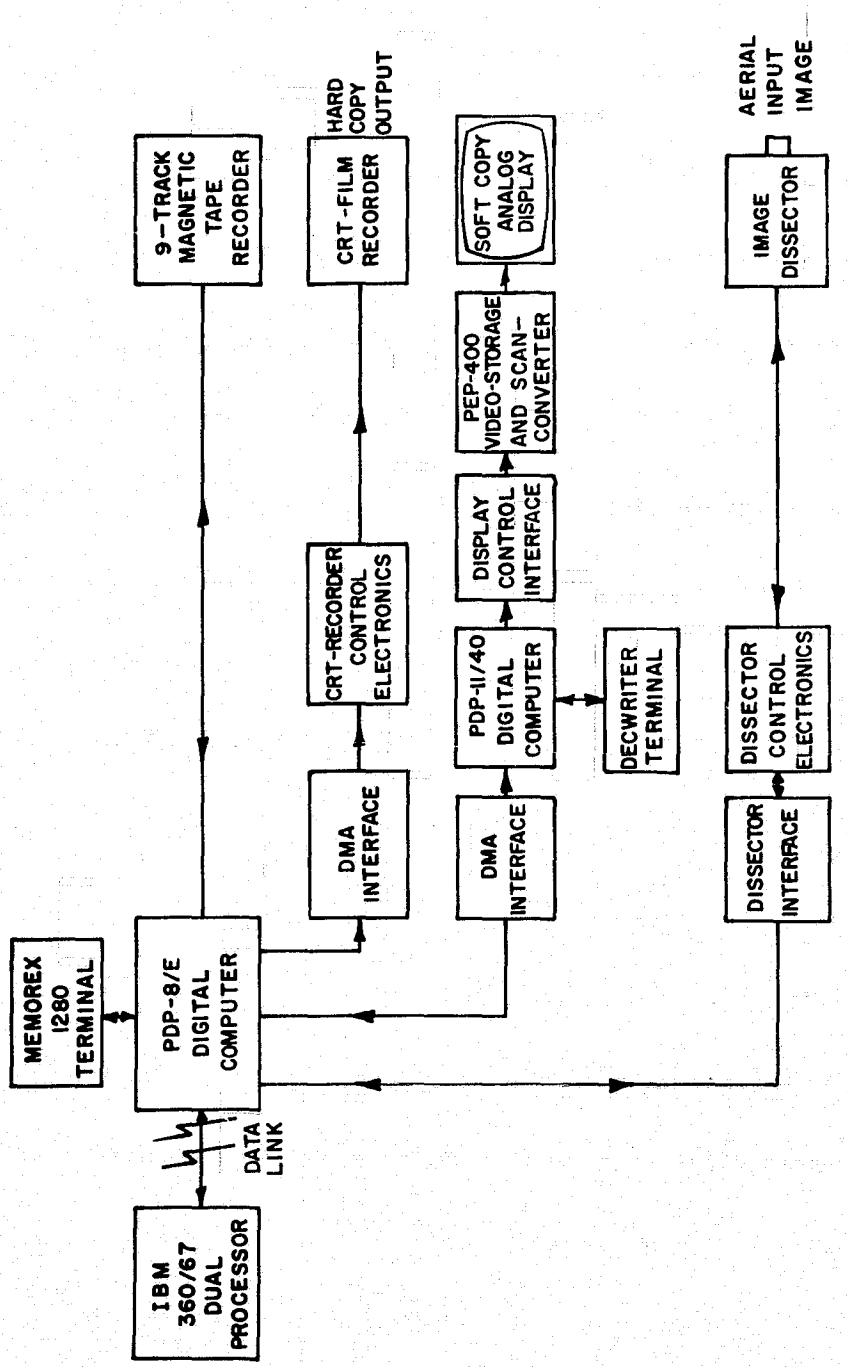

FIGURE 3. IMAGE DISSECTOR AND DIGITIZATION (IDD) FACILITY

photoelectrons by a factor of approximately 5×10^5. The entire electron image is deflected, allowing the aperture to sample different points in the input image.

In the IDD system, the aperture is "scanned" only in the range direction. The aperture is effectively displaced in the azimuth direction as the input film is translated between successive range scans. The dissector aperture used is rectangular, measuring 0.01 mm in the range direction and 0.5 mm in the azimuth direction. The effective width of the azimuth aperture can be reduced by placing a slit of the desired width in the output plane of the optical processor and then reimaging the output on the dissector photocathode surface. The spatial frequency response of the dissector exhibits approximately 40% modulation at 30 line pairs per millimeter.

As shown in Figure 3, the dissector system with its associated control electronics is interfaced to the PDP-8/E minicomputer. This computer buffers a scan line of data from the dissector interface and writes the data on a nine-track, computer-compatible tape system, one line at a time. The images are digitized to eight bits, giving 256 image-intensity levels.

The control electronics enable the user to select the number of picture elements (pixels) digitized per scan line up to a maximum of 3000 per 30-mm scan length. In addition, the scan length can be selected by setting thumb switches to the desired scan-start and scan-stop address or by adjusting the dissector deflection voltages. The integration time per pixel is selectable in increments of 10 μsecs from 10 μsecs to 990 μsecs. (Integration is required to filter

out electron shot noise introduced in the multiplier stages.) Finally, a point skip control allows the user to vary the scan line resolution by skipping up to ten pixels between digitizations. Azimuth sample spacing is determined by the speed of the precision film drive used to translate the input film. The film-drive unit has a long-term stability of 5×10^{-3} per cent and a short-term jitter of less than one micron.

The IDD system is capable of both hardcopy and softcopy display of the digitized data. Hardcopy is provided with a 70-mm CRT film recorder while softcopy is accomplished with a PEP-400 analog scan converter image display interfaced to a PDP-11/40 control computer.

The hardcopy CRT film recorder is interfaced to the PDP-8/E and used for displaying digitized data stored on the magnetic tape unit. The CRT is a fiber-optics, direct-coupled, line-scan recorder capable of recording images up to 3000 elements in range and virtually any length in azimuth (limited by film length). The recording spot size is approximately 20 microns in diameter and recording linearity is ±0.1 per cent in range and ±1 per cent in azimuth. Although not as accurate as the digitization process, this display technique is useful for hardcopy visual presentation of digitized imagery. The CRT film recorder was used to reconstruct the images shown in Section 3 of this report.

2.2 SPATIAL REGISTRATION

The use of a single-channel optical processor can introduce various types and amounts of between-channel geometric distortion in the output imagery. Unless care is

taken, these distortions can include range and/or azimuth scaling errors (magnification errors), image skewing errors, translational errors, and even higher-order image distortions caused by film drive and image dissector scan nonlinearities. The goal in providing the multiband radar imagery described herein was to obtain between-channel registration within several resolution elements (i.e., within about 27 meters). In this case, the higher-order distortions are insignificant.

Sufficient care and precision were utilized in the processor setup to ensure that the scaling and skewing errors were within the stated tolerances. Translational misregistrations were compensated for during the preparation of the interlaced image tapes. Measurements of key road intersections were taken to determine the translation corrections required and to ensure that the registration tolerance was met in the delivered imagery.

Following the processing and digitization procedure, there exist four computer-compatible tapes (CCT's) for each of the image areas (one tape each for X(HH), X(HV), L(HH), and L(HV) radar channels). To determine the amount of translational misregistration between these four images, one must determine the position (tape record number and pixel number within the record) of some prominent geographical feature in all four images. By comparing the coordinates of the feature in all four images, the amount of translation between images is determined.

In the present experiment, computer-generated grayshade plots of the image data were used to determine the location of several prominent road intersections within

each digitized area. The translation correction applied to the images was the average of the translations indicated by the set of registration points. In this manner, registration measurement errors could be minimized. In addition, if the registration error between images is indeed purely translational, then the translation required for all registration points should be the same. Thus, the individual deviations from the average required translation are an indication of both measurement errors and non-translational spatial registration errors. In all cases, the residual registration errors (after translation correction) were less than 30 meters. A total of seven areas from the Phoenix and Huntington imagery were digitized and registered using this procedure.

Because of the different imaging properties of the two wavelengths and two polarizations, it is often difficult to find geographical features which image distinctly in all four channels. Even road intersections are often difficult to pinpoint. Because of this it is recommended that spatial registration reflectors be employed in subsequent radar data collection flights. For each area measuring approximately 4 x 10 km, an array of nine reflectors should be deployed in a rectangular matrix. Each reflector must be constructed so as to be imaged by all four radar channels, and should be deployed in areas of low-clutter return. Clearly distinguishable registration marks would then be produced in all four radar channels and would greatly simplify the registration procedures.

2.3 RELATIVE SIGNAL GAIN IN THE DIGITIZED RADAR IMAGERY

Radar imagery, of the Huntington, Indiana test site and of the Phoenix, Arizona soil moisture test site has been digitized and recorded on magnetic tape for analysis. The relationship between the reflectivity of target objects and corresponding image intensity must be known in order to apply the results of image analysis to the real world. It would be desirable to have a linear and constant transfer characteristic. However, the radar system does not allow such a state. The relationship varies over the image swath due to variations of radar range, antenna gain with depression angle, and signal compression. A number of uncontrolled or unmonitored radar parameters existed in the test flights. These include antenna gain patterns and tilt angles, aircraft roll angle, and recorded signal offset frequency. Even the aircraft altitude above the target area is only coarsely known by barametric altimeter reading.

Estimates of the relative signal gains at swath center and both edges have been made utilizing assumed vertical antenna patterns, theoretical signal compression and integrated gains, free space radiation loss, and computer depression angles. In making these estimates, it is assumed that amplifier gains, transmitter power, recorded signal offset and aircraft roll are all constant.

The estimated signal gain at the swath edges relative to the center was computed along with an estimate of accuracy (see Table 1).

The 13 September 1973 imagery of the Huntington test site was obtained with the radar antennas depressed to place the beam peaks about 15° below the horizon. The

TABLE 1. RELATIVE RESPONSE - ERIM RADAR X- AND L-BANDS

	NEAR EDGE	CENTER	FAR EDGE
SEPTEMBER 13, 1973 - HUNTINGTON, INDIANA TEST SITE, PASSES 2 and 3			
Depression Angle	33^{o}	20^{o}	13^{o}
X-Band	+5.7 dB ± 2 dB	0 dB	-4.4 dB ± 1 dB
L-Band	+0.3 dB ± 1.5 dB	0 dB	-6.9 dB ± 1 dB
APRIL 5, 1974 - PHOENIX ARIZONA N-S PASS, AREAS A AND B			
Depression Angle	49^{o}	40^{o}	34^{o}
X-Band	-0.3 dB ± 2 dB	0 dB	-6.4 dB ± 1 dB
L-Band	0 dB ± 1 dB	0 dB	-4.3 dB ± 2 dB
APRIL 5, 1974 - PHOENIX, ARIZONA E-W PASS, START OF AREA A (Near Guadelupe City)			
Depression Angle	64^{o}	56^{o}	49^{o}
X-Band	-9.3 dB ± 2 dB	0 dB	+3.6 dB ± 2 dB
L-Band	+1.8 dB ± 3 dB	0 dB	-1.8 dB ± 2 dB
APRIL 5, 1974 - PHOENIX, ARIZONA E-W PASS, END OF AREA C (Near Eastern Canal)			
Depression Angle	71^{o}	62^{o}	55^{o}
X-Band	-7.0 dB ± 2 dB	0 dB	+4.6 dB ± 2 dB
L-Band	0.8 dB ± 3 dB	0 dB	-1.3 dB ± 2 dB

importance of the depression angle measurement was not realized at the time of the flight and no accurate measurement was made. Computation of depression angle to the near swath edge appears to have uncertainty of about $\pm 2^{o}$ due to uncertainty of the position of the digitized section of the imaged swath.

The Phoenix flights were made after adjusting the antenna to place the radar beam peaks at 43^{o} below horizontal. Computation of near-edge depression angles is more uncertain at these large depression angles than at smaller angles because a slight error in assumed altitude or slant range represents a large variation of angle. In the E-W flight, the aircraft drifted off course toward the target line (Guadelupe Road) and ran the depression angle up continuously during the pass. Thus, the relative response is given both at the end of Area C (near the Eastern Canal). Between these two points the response should gradually progress linearly with azimuth position from the former to the latter.

2.4 DATA TAPE FORMATS

The basic image storage tape format used in supplying the radar data was the standard LARSYS version 3 format. In some instances, a minor deviation from this format was used. These differences are documented herein. A description of the basic LARSYS-III tape format follows.

There are four types of records on the multispectral image storage tapes. They are

(1) ID Record - 200 full words fixed length
(2) Data Record - variable length
(3) End-of-Tape Records - 200 full words fixed length
(4) End-of-File Records - IBM standard

A multispectral image storage tape contains one or more data runs consisting of an ID record, several Data records, and an End-of-File record. After the last data run on the tape, an End-of-Tape record and two End-of-File records are written on the tape. The physical tape format is IBM nine-track standard with 1600 bits-per-inch density. No system tape leader or trailer records are used.

For purposes of this presentation, a word is defined as 32 bits and a byte as eight bits. Details regarding the record formats follow.

ID Record. The run identification record is the first record of each data run and, thus, the first record of a data tape. The record is 200 words fixed length and each word has the following definitions:

Words	Word Type	Description
ID(1)	Integer	LARS Tape Number (e.g., 1, 17, 102, etc.)
ID(2)	Integer	File number on this tape
ID(3)	Integer	Run number (8 digits-aabbbbcc) aa - last two digits of the year data was taken bbbb - running serial number for the year data was taken cc - unique digits for runs which would otherwise have the same run number
ID(4)	Integer	Continuation code ID(4) = 0 means the first line of the run follows this ID record

Words	Word Type	Description
		ID(4) = X means that the data following this ID record is a continuation of a run started on tape X
ID(5)	Integer	Number of data channels (spectral bands) on tape (in this case two or four)
ID(6)	Integer	Number of data samples per channel per line (must be an even multiple of four)
ID(7-10)	Alphanumeric (4A4)	Flight line identifications (16 characters)
ID(11)	Integer	Month data was taken
ID(12)	Integer	Day data was taken
ID(13)	Integer	Year data was taken
ID(14)	Alphanumeric (1A4)	Time data was taken (local, military)
ID(15)	Integer	Altitude of sensor platform (feet)
ID(16)	Integer	Ground heading of sensor platform
ID(17-19)	Alphanumeric (3A4)	Date data run was generated on this tape (12 characters-mmmm, dd, yyyy mmmm - month dd - day yyyy - year
ID(20)	Integer	Number of data records in the run
ID(21-50)	Integer	All zero (to be defined later)
ID(51)	Real	Lower limit in micrometers of first spectral band on tape (3.0×10^5 for X-band, 2.5×10^6 for L-band)
ID(52)	Real	Upper limit in micrometers of first spectral band on tape [in this case, same as ID(51)]

Words	Word Type	Description
ID(53-55)	Real	Not applicable (all set to 0.0)
ID(56-200)	Real	Repeat of ID(51-55) for ID(5) channels in order of appearance in Data records
ID(51-200)	Real	= 0.0 if data channels do not exist

Data Record. The data records for a run follow the run ID record and comprise the text of the data run. Each data record is a physical record block on the tape and contains the data samples for ID(5) (see ID record) channels for one scan line. The first half-word (bytes 1 and 2) of each record is the data record number, where the first data record has number one. The second half-word (bytes 3 and 4) will be the remote sensing platform roll parameter indicating relative position of the roll of the platform for this line of data. Since the roll parameter is not known, it has been set to 32,767.

The fifth byte of the data record is the first data sample from the first channel. The sixth byte, the second sample from channel one and so on through ID(6) samples and ID(5) channels. Thus, byte 4+2*ID(6)+1 is the first sample of channel three and each data record of a given run is 4+ID(5)*ID(6) bytes long.

The data samples of each channel are from the field of view of the sensor, except the last six. The last six are usually used as calibration sources for multispectral data in the visible and near-visible spectrum. For the radar data, the calibration values are not applicable and are therefore all set equal to 0.0.

Data sample values are in the range of 0 to 255 (eight bits) with no sign bit. Zero represents low relative radar reflectivity and 255 indicates high or saturated radar response.

End-of-Tape Record. The end-of-tape record is similar to the ID record containing 200 full words. The word definitions are:

Words	Word Type	Description
ID(1)	Integer	LARS tape number
ID(2)	Integer	File number on this tape
ID(3)	Integer	Set equal to 0
ID(4)	Integer	Continuation code ID(4) = 0 means end of data ID(4) = X means data in previous file is continued on tape X
ID(5-50)	Integer	All zero (may be defined later)
ID(51-200)	Real	0.0 (may be defined later)

For the Phoenix radar data which were shipped to NASA/JSC, there is a slight discrepancy in the tape format used. For those data tapes, the data-sample count supplied as word ID(6) was used to indicate the number of data samples per channel per line, not including the six calibration data values. The correct LARSYS-III format dictates that this count is to include the six calibration data values. Thus, for the NASA Phoenix tapes, the number stored in word ID(6) is six less than it should be according to standard LARSYS documentation. This fact must be taken into account when utilizing the data types. The Huntington data tapes adhere correctly to the standard LARSYS-III format.

2.5 SUMMARY OF DATA SUPPLIED

A summary of the data which has been processed, digitized, registered, and shipped to NASA/JSC is given in Table 2. The areas covered by the Huntington radar data are shown in Figure 4.

With respect to the Huntington data, only L-band imagery has been digitized, registered, and interlaced on the LARSYS tape. The two channels of X-band imagery collected are not acceptable for digital processing and have, therefore, been omitted. Two problems occurred during the data collection flight causing X-band image degradations and making the digitized data relatively useless for meaningful processing. The first problem encountered was an interface failure between the aircraft inertial navigation system (INS) and the two signal film drives. Normally, velocity information supplied by the INS is used to control the speed of the film drives. When this linkup failed during the flight, a manual override technique was adopted which consisted of continually observing the aircraft's airspeed indicator and manually adjusting the speeds of the two film drives. Each film drive must be adjusted individually since one must run slower than the other to account for differences in radar wavelength. Since the adjustment was done manually and was, at best, only approximate, azimuth spatial distortions occur in the imagery from all four channels. Since both polarization configurations for a single wavelength are recorded on a single drive, the two channels for each wavelength can be registered to one another. However, the X-band imagery cannot be registered to L-band using techniques available at ERIM since the relative distortion between film drives is unknown. Thus,

TABLE 2. SUMMARY OF DIGITAL MULTIBAND RADAR IMAGERY SUPPLIED TO NASA/JSC

Data Item (Date Shipped)	Area Description	Image Size (Pixels)	Scanning* Aperture Size (m)	Pixel* Spacing (m, R&A$_z$)	Radar* Resolution (m)	Number of Channels
Phoenix N-S Pass Area A (8 November 1974)	1/2 mile on either side of 91st Street from south of Thomas Road to Peoria Avenue	948 x 5946	2.03 x 2.03	2.03 x 2.03	9.14 x 9.14	4
Phoenix N-S Pass Area B (8 November 1974)	1/2 mile on either side of the Salt River to Thomas Road	960 x 5970	2.03 x 2.03	2.03 x 2.03	9.14 x 9.14	4
Phoenix E-W Pass Area A (6 December 1974)	1/2 mile on either side of Quadalupe Road from west of Interstate 10 to east of Alma School Road	876 x 5955	2.03 x 2.03	2.03 x 2.03	9.14 x 9.14	4
Phoenix E-W Pass Area B (6 December 1974)	1/2 mile on either side of Quadalupe Road from west of Anzona Avenue to east of the Eastern Canal	896 x 5606	2.03 x 2.03	2.03 x 2.03	9.14 x 9.14	4
Phoenix E-W Pass Area C (6 December 1974)	1/2 mile on either side of Quadalupe Road from west of Eastern Canal to east of Sossaman Road	932 x 3417	2.03 x 2.03	2.03 x 2.03	9.14 x 9.14	4
Huntington Pass 2 (16 January 1975)	(see Figure 8)	1014 x 7078	2.03 x 2.03	4.06 x 4.06	9.14 x 9.14	2
Huntington Pass 3 (15 January 1975)	(see Figure 8)	1014 x 8000	2.03 x 2.03	4.06 x 4.06	9.14 x 9.14	2

*All measurements given in meters with respect to slant range plane.

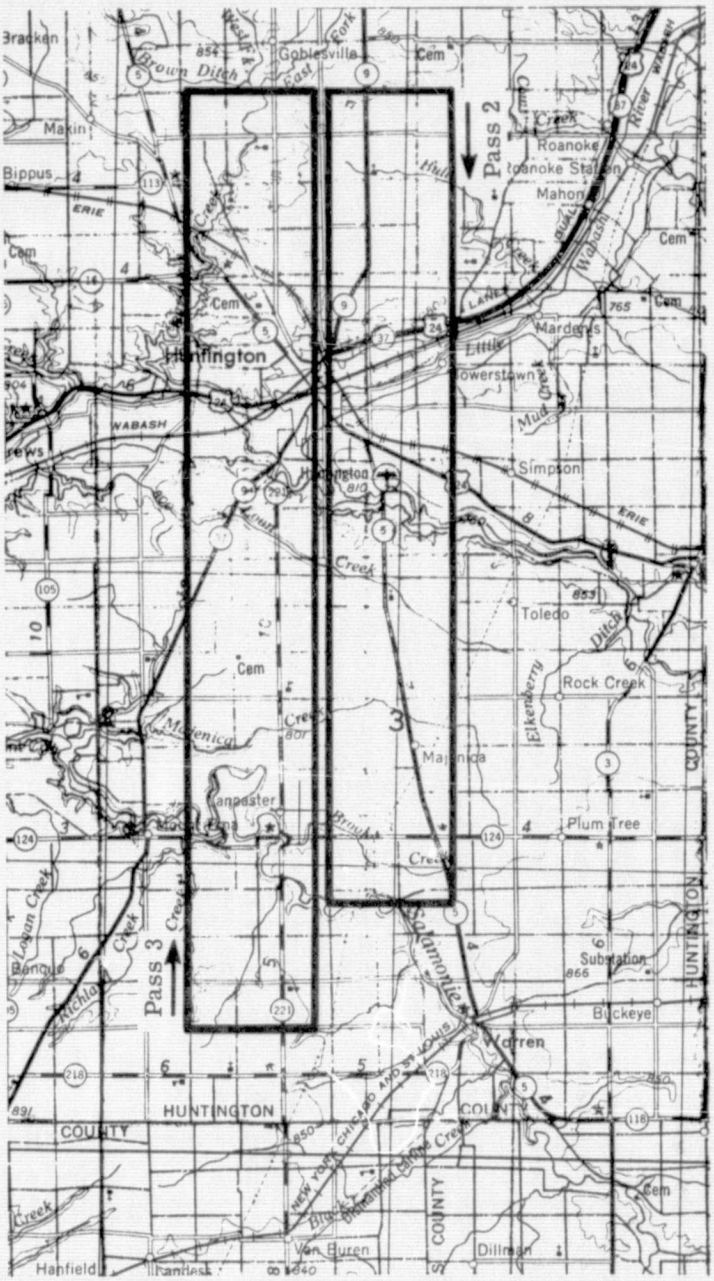

FIGURE 4. AREAS OF RADAR COVERAGE DIGITIZED FROM HUNTINGTON, INDIANA TEST SITE

at best, only two sets of two-channel registered imagery could be used.

The second problem encountered seems to preclude use of the X-band imagery altogether. It was discovered after the flight that an X-band antenna-wander problem occurred. Apparently the antenna gimbal allowed the antenna to experience pointing errors in azimuth direction. These pointing errors cause the energy in the Doppler frequency spectrum to periodically shift up or down in frequency. This causes the azimuth spectrum in the processor to "wander" in and out of the processing aperture which, in turn, causes intensity striations to transverse the image in the range direction. At times this phenomena causes intensity drops of from 3- to 8-dB. Because of this degradation, the image intensities cannot be taken literally to represent the strength of radar returns and, hence, are relatively meaningless for digital processing applications. Therefore, it was decided not to incur the expense of digitizing and registering the two X-band channels. Photographic reproductions of the X-band imagery have been supplied to Kansas for their visual analysis, however. The image striations are evident in the portion of X-band imagery shown in Figure 5.

An additional effort has been made to supply radar data to the University of Kansas directly. Kansas does not have the equipment to read the 1600-bpi tape densities as supplied by ERIM via NASA, so an attempt has been made to supply them with data in a 800-bpi tape format. This was done to save Kansas a two- to three-week delay in having the tapes converted on equipment located at Wichita State

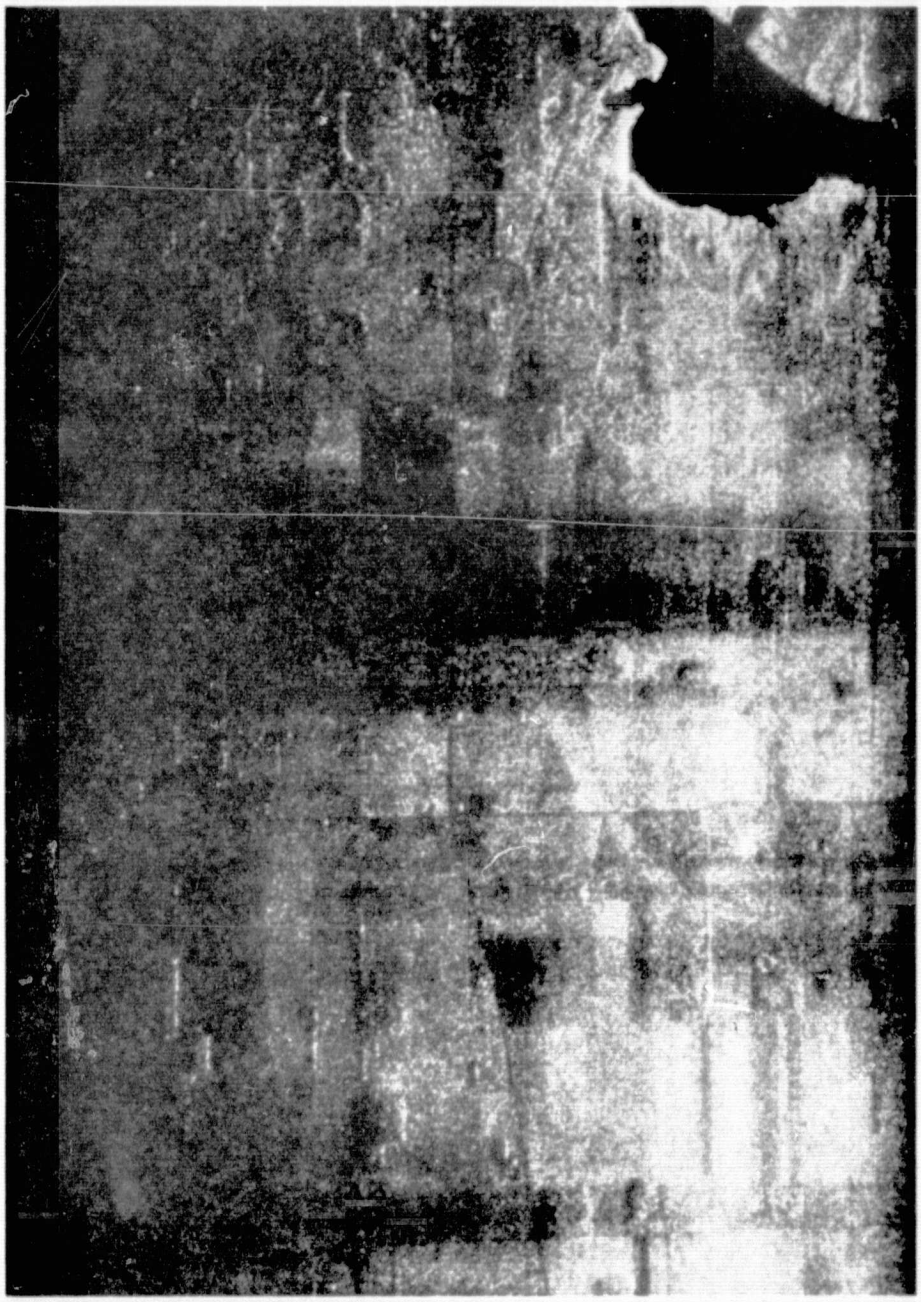

FIGURE 5. HUNTINGTON RADAR IMAGERY SHOWING STRIATIONS CAUSED BY ANTENNA POINTING ERRORS. 3.2 cm wavelength, like-polarization.

University. The following data has been supplied directly to Kansas:

Data Item	Data Shipped or Delivered
(1) Phoenix, (N-S pass) preliminary, 1 area, 3 channels each	23 October 1974
(2) Phoenix (N-S pass) 2 areas, 4 channels (MTS copy)	8 November 1974
(3) Phoenix (N-S pass) 2 areas, 4 channels each (MTS copy)	Hand-delivered 27 December 1974
(4) Phoenix (N-S pass) 2 areas, 4 channels each (PDP-11 copy)	Hand-delivered 27 December 1974
(5) Phoenix (E-W pass) 3 areas, 4 channels each (PDP-11 copy)	13 January 1975
(6) Huntington (Passes 2 and 3) 2 channels each (PDP-11 copy)	17 January 1975

Upon the second shipment of data to Kansas, tape compatibility problems began to occur. The Kansas University Computer Center could not read the tapes generated on the Michigan Computer System (MTS) without an unacceptable number of parity errors occurring. Some test tapes were exchanged which led to the belief that the tapes were somehow picking up bit errors in transit between ERIM and Kansas University. To further isolate the problems, two more sets of the Phoenix N-S data were hand-delivered to Kansas University on 27 December. One of these sets was generated on MTS, while the second was a copy of the first made on ERIM's PDP-11/45 computer facility. ERIM experienced no problems in reading the MTS version to make the copy.

Upon trying the tapes, Kansas found that they could acceptably read the PDP-11/45 versions, but still could not successfully assess the data on the second set of MTS tapes. At this point, it was decided to generate all future data for Kansas on MTI and then make additional copies on ERIM's PDP-11/45 facility. The remaining two shipments (Phoenix E-W and Huntington) were sent as PDP-11 copies.

3
PRELIMINARY DATA PROCESSING

The resources available following the preparation and shipment of the required digital image data permitted only a preliminary analysis of portions of the image data. Both univariate and multivariate statistical analysis has been applied to fields which exhibited various surface conditions during the data collection cycle. The results, though limited in extent, have shown that there is high correlation between soil moisture content and the multiband radar returns, at least for the extreme ends of the moisture spectrum. However, other surface conditions such as surface roughness, furrow orientation, and vegetation type and coverage appear to have equally significant effects upon the multiband radar returns. Thus, future analysis efforts must be directed towards determining those surface characteristics which have the dominant effect upon the radar signatures and developing techniques for isolating the effects of the surface conditions which are to be measured.

The use of digitized radar data for earth science applications is a relatively new endeavor. Consequently, although much experience has been gained through the employment of digital analysis of multispectral scanner imagery, it is still uncertain if there is a high degree of transference of these analytical techniques from the one data system to the other. It is apparent that the multispectral radar which was employed during the Phoenix Soil Moisture Test (5 April 1974) has a high potential for quantitatively detecting variations of the earth's surface. The exact interpretation and the ultimate application of these

data are, however, still quite speculative because a detailed, thorough, and complete analysis has not been conducted. The nature of the detected variations also continues to be under investigation. The next section will describe those areas selected for analysis.

3.1 SELECTION OF FIELDS FOR ANALYSIS

Because of the limited resources available, the number of fields to be analyzed had to be restricted. To minimize the tape handling expenses involved, the fields selected were all chosen to lie within a single, digitized area; in this case the Phoenix North-South pass, Area A data tape was selected. Within that data set, it was further decided to analyze a set of fields which were situated along a line of constant slant range in order to minimize the need for correction of the range-dependent target amplitude effects discussed in Section 2.3.

The fields immediately adjacent to 91st Street in the N-S pass were ruled out for analysis since the radar returns in the majority of those fields were corrupted by small signal "capture" effects. These effects are caused by radar system saturation in the presence of extremely large radar returns. The uncompressed radar signal saturation virtually erases the small signals from neighboring areas, causing the disappearance of small returns (e.g., clutter) in the vicinity of extremely strong returns, such as those returns from the "dihedral-like" sides of the irrigation canals which parallel 91st Street. Thus, the fields chosen for analysis were restricted to those more than 1/4 mile from 91st Street.

The fields actually chosen are delineated in Figure 6 using the NASA-assigned field numbers. The six fields originally selected were numbers 38, 42, 51B, 60B, 97, and 99B. Visual analysis of same-day IR color aerial photography revealed that the ground-truth information for field 60B was incomplete. It was determined that approximately 1/3 of the field had been recently irrigated and exhibited small pools of standing water in the extreme bottoms of the furrows. The remainder of the field appeared to have remained dry so it was assumed that the recorded ground-truth information still applied to that portion of the field. To permit analysis of the two surface conditions exhibited within the otherwise homogeneous field, the radar data were further divided into a wet portion (renamed field No. 60C) and a dry portion (still labeled field No. 60B). A summary of the ground-truth information available for the selected fields appears in Table 3.

3.2 VISUAL ANALYSIS

After selection for analysis, the individual fields were assessed visually using the four-channel radar digital imagery, and the "same-day" aerial photography coverage (both B&W and color IR). The intention was to isolate any anomalies in the selected data which might affect the processing results. It was this visual analysis which provided the "discovery" of the wet portion of NASA field No. 60B. One mode of visually assessing the four-channel radar imagery is by the use of CRT film recordings of the digitized data. Figure 6 was produced in this manner with the field boundaries inserted into the image by the computer.

TABLE 3. SUMMARY OF GROUND TRUTH FOR FIELDS SELECTED FOR ANALYSIS

	PERCENT MOISTURE								
	Depth (cm)					Rows			
	1.0	2.0	5.0	9.0	15.0	Veg	N/S	E/W	BARE
38	1.50	1.96	6.38	10.22	12.45	-	X	-	X
42	1.30	2.08	7.78	11.20	13.19	-	X	-	X
51B	1.85	2.33	3.83	5.77	7.81	-	X	-	X
60B	1.4	2.10	4.36	8.35	10.99	-	-	X	X
60C	-	-	-	-	-	-	-	X	X
97	-	-	-	-	-	100%	X	-	-
99B	3.2	7.77	15.88	19.00	20.73	-	X	-	X

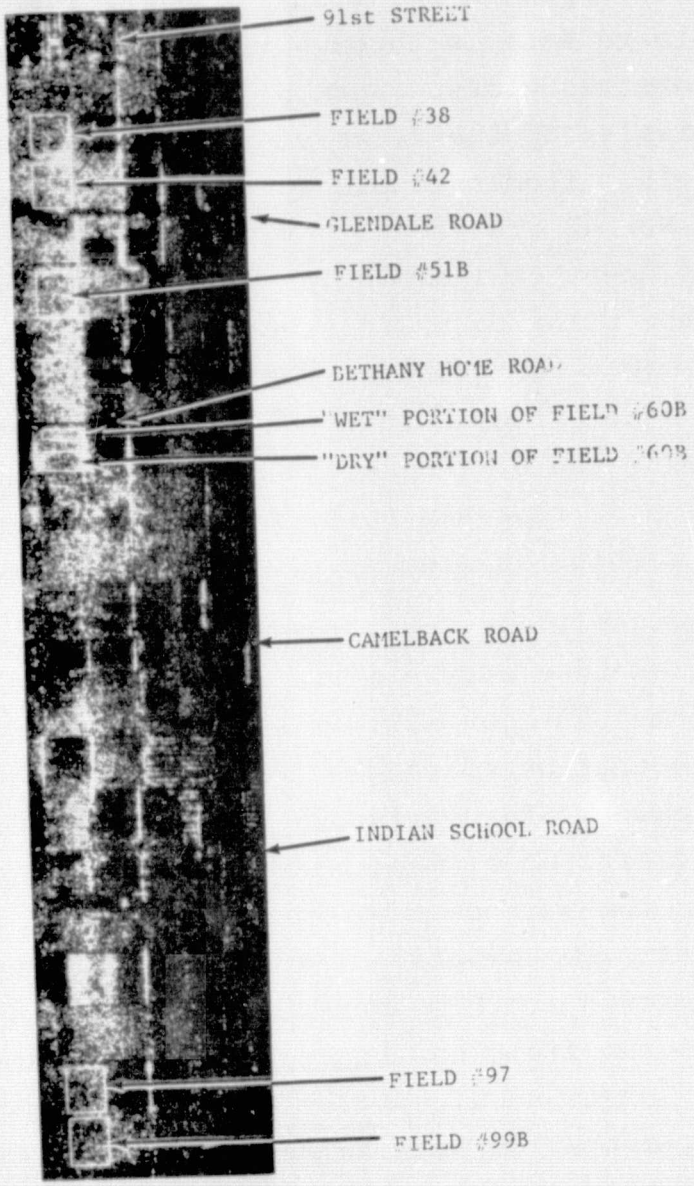

FIGURE 6. DIGITAL RADAR IMAGE FROM PORTION OF NASA PHOENIX AGRICULTURAL TEST SITE, 5 APRIL 1974. X-band, parallel polarization.

An alternate approach for visually analyzing the four-channel radar image data is through the use of three-dimensional isometric plots. Such plots provide a more quantitative display of the relative radar intensities within each field. Isometric plots of the two X-band channels for field No. 42 are shown in Figures 7 and 8, respectively. Adjacent cell averaging (5 x 5) was applied to the radar data prior to making the isometric plots. This averaging makes the sampling resolution roughly equivalent to the radar system resolution (roughly 9m x 9m). Thus, in Figures 7 and 8, the height of each intersection of lines in the plot represents the average radar return within a radar resolution element.

It is immediately apparent from the isometric plots that the radar response over a given field is far from homogeneous. Some, but not all, of the radar response variation can be attributed to the coherent radar system clutter or "speckle." The variances whose extent is larger than a single resolution element must be attributed to inhomogeneities in the surface condition of the field itself. The appearance of such variations leads one to question whether or not ground-truth measurements made at isolated positions within the field can be expected to accurately represent other locations within the fields. Further analysis and experimentation will be required to determine the viability of the ground-truthing procedures.

3.3 COMPUTER ANALYSIS

The initial analysis efforts were directed towards univariate statistical analysis of individual channels for individual fields. The simplest procedure applied was to

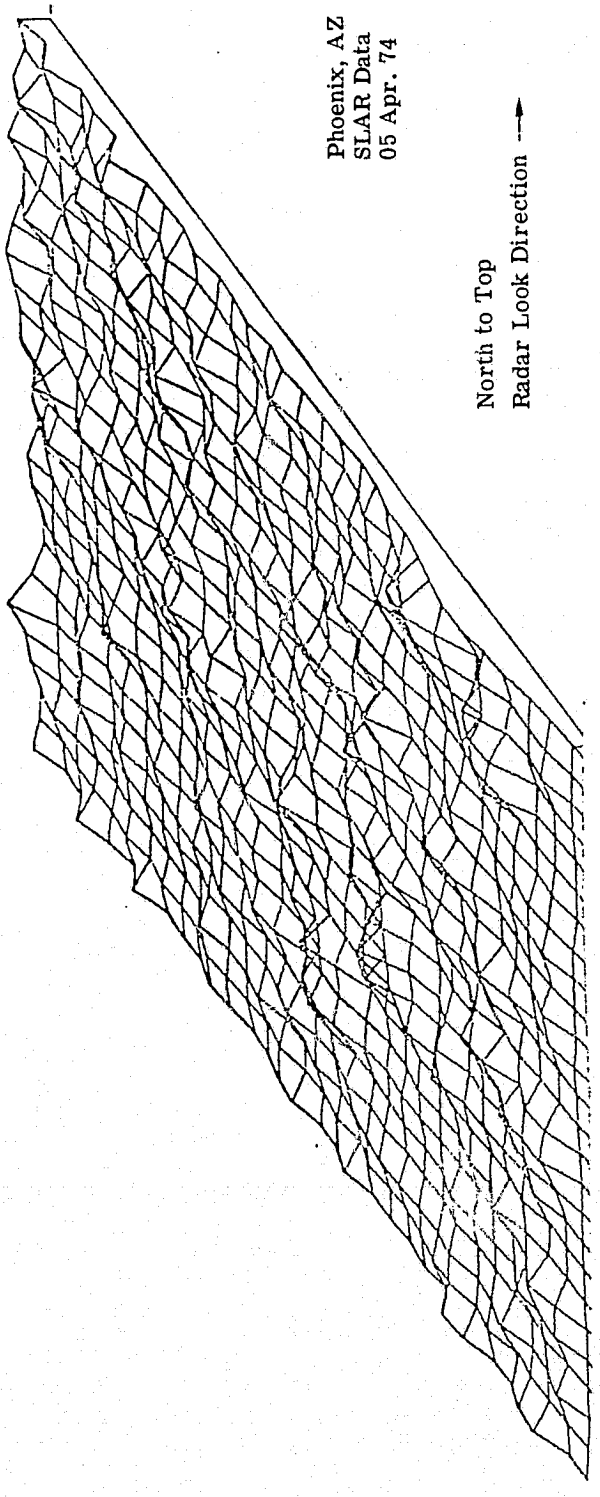

FIGURE 7. ISOMETRIC PLOT OF X(HH) FOR FIELD NO. 42

FIGURE 8. ISOMETRIC PLOT OF X(HV) FOR FIELD NO. 42

calculate the means and standard deviations within the individual fields. In some cases, a single radar channel was useful for delineating soil surface conditions.

As an example, consider the univariate statistics calculated for the wet (60C) and dry (60B) areas as shown in Table 4 which indicate that there is a fair amount of separability between the wet and dry areas with respect to the L(HV) channel. For this case, the distance between the means is greater than either of the within-field standard deviations. The rather large standard deviations may be attributed to the coherent radar system clutter effects. If one can reduce the system clutter without appreciably affecting the average radar returns, then better class separability can be obtained.

Adjacent cell averaging (a form of non-coherent integration) is one technique for reducing system clutter variance. Adjacent cell averaging is the process of using the average value of a set of neighboring pixels to represent the radar return from the corresponding larger area. This has the effect of reducing the variance of the coherent radar system clutter while not affecting the average strength of returns. (One should also remember that there is a loss in radar resolution in this case which will affect the ability to accurately determine the boundaries between areas exhibiting different surface conditions.) The net effect should be an increase in the separability between data classes.

Adjacent cell averaging of 5 x 5 and 10 x 10 were applied to the extracted field data. The effect of these operations upon the univariate statistics is apparent in

Tables 5 and 6 for adjacent cell averages of 5 x 5 and 10 x 10, respectively. In general, the means remain approximately the same for each field, while the variances decrease as expected. (Theoretically, the means should be exactly the same, but the dimensions of the original areas in terms of pixels were not always integer multiples of 5 or 10. Consequently, slightly different areas are being analyzed for the various amounts of adjacent cell averaging.) In order to test the separability of the wet and dry areas as a function of adjacent cell averaging, a linear discriminant decision rule was derived and tested.

A linear discriminant analysis algorithm was applied to the four-channel data extracted from the wet and dry areas. The discrimination was made on a pixel-by-pixel basis. Each pixel is comprised of four numbers representing the returns from the four radar channels. The ground area covered by a pixel is determined by the aperture size used in the digitization procedure. In this case a pixel covers a 2 x 2 m slant range area. The actual radar resolution for this data was purposefully limited to 9 x 9 m (allowing DoD declassification of the data), so the unaveraged digital image data is oversampled by approximately 4.5 in both coordinates. The results of the discriminant analysis on the raw data are shown in Table 7.

The discriminant analysis algorithm arrived at a decision rule which classified 2616 of the 3900 wet pixels as belonging to the wet class, and 7690 of the 8580 dry pixels as belonging to the dry class, for an overall percentage correct classification of 82.6.

TABLE 4. STATISTICS FOR WET VS. DRY AREAS (UNAVERAGED)

AREA	CHANNEL	NO. PIXELS	MEAN	STD. DEVIATION
Wet (60C)	X(HH)	3900	40.9	32.6
	X(HV)	3900	51.9	43.3
	L(HH)	3900	78.6	57.5
	L(HV)	3900	121.0	72.3
Dry (60B)	X(HH)	8580	45.9	37.6
	X(HV)	8580	33.5	32.9
	L(HH)	8580	54.8	46.6
	L(HV)	8580	40.8	38.3

TABLE 5. STATISTICS FOR WET VS. DRY AREAS
(5 x 5 AVERAGING)

AREA	CHANNEL	NO. OF PIXELS	MEAN	STD. DEVIATION
Wet (60C)	X(HH)	182	42.0	27.6
	X(HV)	182	49.6	29.0
	L(HH)	182	76.9	42.0
	L(HV)	182	126.0	43.5
Dry (60B)	X(HH)	338	45.5	27.1
	X(HV)	338	32.9	25.3
	L(HH)	338	54.8	36.2
	L(HV)	338	40.3	28.1

TABLE 6. STATISTICS FOR WET VS. DRY AREAS
(10 x 10 AVERAGING)

AREA	CHANNEL	NO. OF PIXELS	MEAN	STD. DEVIATION
Wet (60C)	X(HH)	39	40.4	15.3
	X(HV)	39	51.5	21.5
	L(HH)	39	78.1	33.3
	L(HV)	39	121.0	25.3
Dry (60B)	X(HH)	78	44.8	17.2
	X(HV)	78	31.7	14.0
	L(HH)	78	54.9	27.9
	L(HV)	78	39.2	21.0

TABLE 7. LINEAR DISCRIMINANT ANALYSIS OF WET VS. DRY AREAS USING UNAVERAGED FOUR-CHANNEL RADAR DATA [X(HH), X(HV), L(HH), L(HV)]

True Class	Decision Class		Percentage Correct (%)
	Wet	Dry	
Wet	2616	1284	67.1
Dry	890	7690	89.6
Overall Percentage Correct: 82.6			

TABLE 8. LINEAR DISCRIMINANT ANALYSIS OF WET VS. DRY AREAS USING (5 x 5) AVERAGED FOUR-CHANNEL RADAR DATA

True Class	Decision Class		Percentage Correct (%)
	Wet	Dry	
Wet	157	25	86.3
Dry	24	314	92.9
Overall Percentage Correct: 90.6			

When adjacent cell averaging was applied to the data, even more encouraging results were obtained. As in the univariate analysis, the effect is to reduce the within-class variance without altering the means, thereby obtaining better separability between classes. The increase in performance is evident in the results shown in Tables 8 and 9 for adjacent cell averaging of 5 x 5 and 10 x 10, respectively.

In order to better estimate the performance of the linear discriminant analysis, additional areas were classified using the previously derived decision rule. These areas, indicated in Figure 2, were all considered to be in the dry class (moisture content less than 16% to a depth of 5 cm). No other ground-truthed fields within the selected area were moist enough to be called wet. (The selected fields were all located at the same slant range to prevent system gains which are a function of range from altering the results.) Thus, five additional fields were added to the set of data subjected to the linear discriminant rule (these fields were not used to derive the rule). The results of the analysis appear in Table 10. As can be seen from the table, the inclusion of testing data does not significantly decrease the performance of the classifier.

These preliminary results indicate that the multiband radar image data can be related to soil moisture content, at least at the extreme ends of the moisture spectrum. Further analysis is required to determine if this correction holds over the entire moisture spectrum or whether the moisture related effects are dominated by the effects of other "extraneous" surface conditions such as roughness or vegetation.

TABLE 9. LINEAR DISCRIMINANT ANALYSIS OF WET VS. DRY AREAS USING (10 x 10) AVERAGED FOUR-CHANNEL RADAR DATA

True Class	Decision Class		Percentage Correct (%)
	Wet	Dry	
Wet	38	1	97.4
Dry	5	73	93.6
Overall Percentage Correct: 94.9			

TABLE 10. TESTING OF LINEAR DISCRIMINANT ANALYSIS USING (10 x 10) AVERAGED FOUR-CHANNEL RADAR DATA

True Class	Decision Class		Percentage Correct (%)
	Wet	Dry	
Wet	38	1	97.4
Dry	84	1024	92.4
Overall Percentage Correct: 92.6			

Future efforts should also examine the use of self-normalizing techniques which minimize the requirements for radar system calibration. Lack of sufficient calibration information may require that the radar image data be considered not as absolute values, but as relative values between radar channels. To this end, serious consideration should be given to ratios and other transforms of the data which result in quantities which are insensitive to absolute radar response. Examples of such operations are:

(1) X(HH)/X(HV)
(2) L(HH)/L(HV)
(3) X(HH) - X(HV)
(4) L(HH) - L(HV)
(5) X(HH) - X(HV)/L(HH) - L(HV)
(6) X(HH) - X(HV)/L(HH) - L(HV)

In which X(HH) is the uncalibrated backscatter for X-band, parallel-polarized energy; and similarly for X(HV); L(HH); L(HV).

Figure 9 shows the cumulative distributions of one such variable [L(HH)/L(HV)] for the set of field data which has been discussed herein. Some obvious groupings occur in the data, although the physical characteristics giving rise to the groups have yet to be fully determined. The extremely wet area (60C) does separate out, however. The groupings are interesting enough to warrant further study.

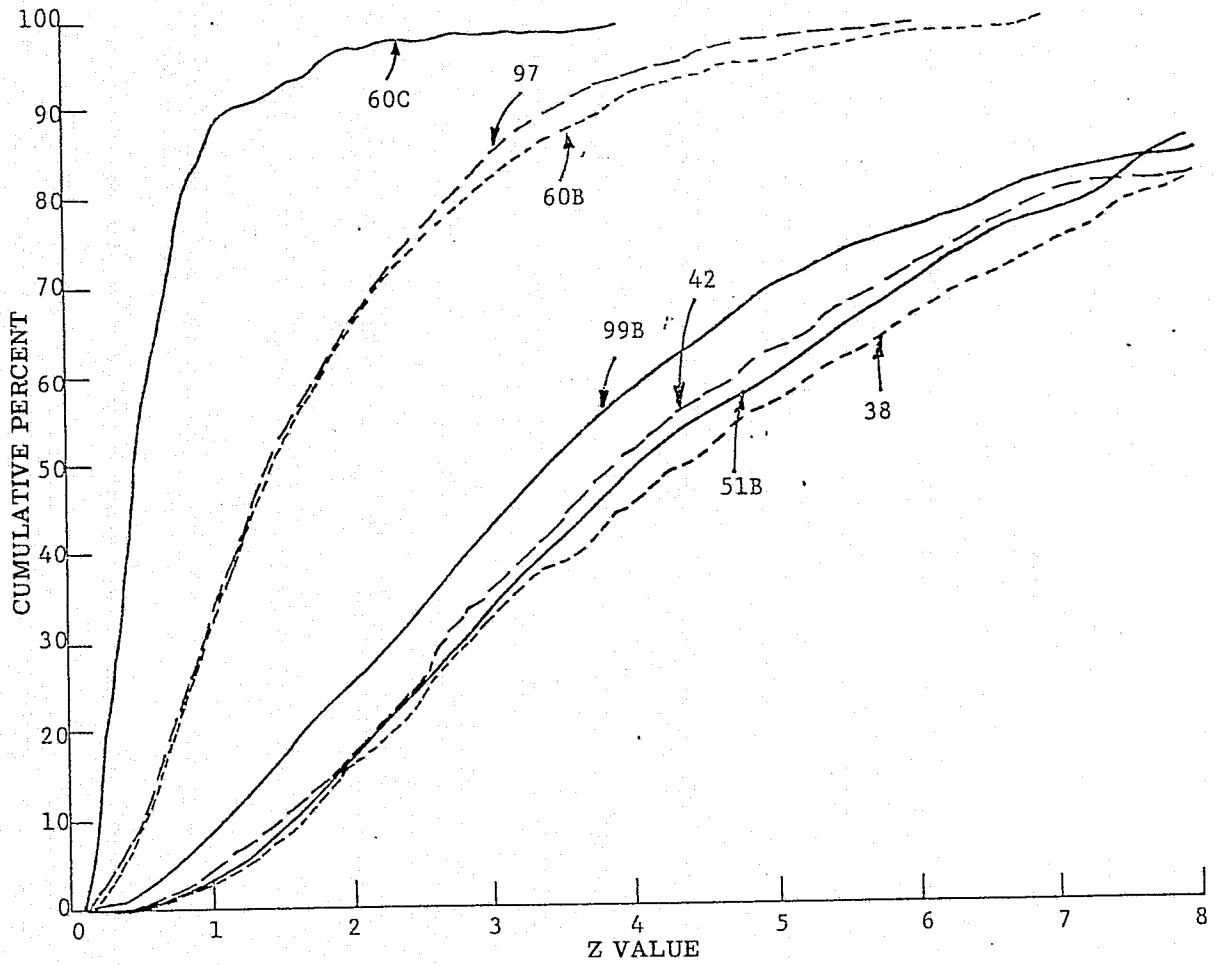

FIGURE 9. CUMULATIVE DISTRIBUTIONS OF SAR DATA. Ratio: L(HH)/L(HV)

4
SUMMARY AND RECOMMENDATIONS

Approximately 137 square miles (statute) of ERIM dual-polarization X- and L-band radar imagery has been digitized, spatially registered, and tape formatted for transmittal to NASA/JSC and the University of Kansas. Imagery corresponding to both the Phoenix, Arizona and Huntington, Indiana test sites was provided. Due to the failure of portions of the airborne radar system, only L-band imagery (like- and cross-polarized) could be provided for the Huntington agricultural test site.

Post-processing registration of the digitized four-channel imagery was difficult due to the lack of clearly identifiable homologous image points. Because of the different imaging properties of the two wavelengths and polarizations, it is difficult to find geographical features (for use as registration points) which image distinctly in all four channels. To simplify the registration process, it is recommended that spatial-registration reflectors (visible in all four channels) be employed in subsequent radar data collection flights.

Additional thought should be given to the choice of quantization levels when converting the radar image intensities to 256 shades of gray. To avoid severe saturation of strong returns from man-made objects, the data presented herein was digitized in a manner which forced the majority of returns from the fields to fall into about 32 quantization levels. Conversations with the users* of the data

*Dr. Fawaz T. Ulaby, the University of Kansas, Remote Sensing Laboratory, personal communication.

indicate that this number of levels in the data range of interest may be insufficient. Finer-intensity quantization of the returns from fields could be easily obtained (at the expense of cultural target saturation) by employing a logarithmic amplifier prior to A/D conversion of the dissector camera video.

Multivariate statistical analysis and discrimination was applied to portions of the Phoenix radar image data to determine separability as a function of soil moisture content. Preliminary results indicate that the multiband radar image data can be related to soil moisture content, at least the extreme ends of the moisture spectrum. Further analysis is required to determine if this correlation holds over the entire moisture spectrum or whether the moisture related effects are dominated by the effects of other "extraneous" surface conditions such as roughness or vegetation.

The most detrimental aspect of the digital SAR data produced to date is the lack of adequate system calibration. Ones ability to detect and quantify field surface conditions is greatly limited by the loose tolerances associated with our current knowledge of the range response of the radar. In analyzing the data, intensity trends were noticed which could not be adequately explained by the calibration data described earlier (Table 1). Thus, the analysis described in this report was limited to data occupying a relatively small range.

Such an approach places an unacceptable restriction on the use of the data. Thus, ERIM recommends that the necessary equipment be built and procedures established to ensure the best possible SAR system calibration for future radar remote-sensing missions.

REFERENCES

1. W. M. Brown, "Synthetic Aperture Radar," IEEE Trans. on Aerospace and Electronic Systems, AES-3, March 1967, pp. 217-229.

2. W. M. Brown and L. J. Porcello, "An Introduction to Synthetic Aperture Radar," IEEE Spectrum, Vol. 6, No. 9, September 1969, pp. 52-62.

3. E. N. Leith, "Quasi-Holographic Techniques in the Microwave Region," Proceedings of the IEEE, Vol. 59, No. 9, September 1971, pp. 1305-1318.

4. A. Kozma, E. N. Leith, and N. G. Massey, "Tilted Plane Optical Processor," Appl. Opt., Vol. 11, No. 8, August 1972, pp. 1766-1777.